Compliant In-Hand Multifingered Rolling Using Tactile Sensing

Huan Weng and Kevin M. Lynch

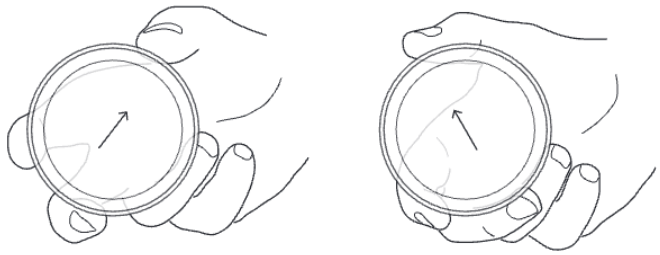

Fig. 1: Most types of in-hand manipulation require rolling and/or twisting at the finger contact patches, such as this example of in-hand turning of a cylinder.

***Abstract*—We investigate in-hand rolling manipulation using a multi-fingered robot hand where each finger is equipped with a Visiflex, a compliant tactile fingertip sensor providing contact location and wrench information. Each fingertip is hemispherical, allowing it to roll, spin, and slide on the object. We derive the equations of motion for compliant quasistatic in-hand rolling manipulation, and we formulate a fingertip rolling controller for multiple fingers to achieve desired object rolling motion in a grasp. The controller is tested experimentally on object spinning and screwing tasks.**

***Index Terms*—Tactile sensing, compliance, in-hand manipulation, contact mechanics**

I. Introduction

We study in-hand rolling manipulation using a multi-fingered robot hand, where each finger is equipped with our Visiflex tactile fingertip [1]. The Visiflex is designed to achieve 1) well-characterized compliance at the fingertip, 2) contact location sensing at the fingertip, and 3) 6-dof contact wrench sensing, and its hemispherical shape allows rolling manipulation, which is impossible with tactile sensors with a largely flat profile. All these make it possible for us to build on our previous work on sliding regrasp, extending to the case where the fingertip is a hemisphere (not a point) and the motion-controlled finger "anchor" has six degrees of freedom and is connected to the fingertip via a 6-dof flexure, unlike the 3-dof anchors and flexures of [2]. The real-time wrench and contact location feedback, coupled with control strategies that will be explored in this paper, enable robust execution of various in-hand rolling manipulations, such as rotating a cylinder, as shown in Figure 1.

Huan Weng and Kevin M. Lynch are with the Center for Robotics and Biosystems and the Department of Mechanical Engineering, Northwestern University, Evanston, IL 60208, USA. Kevin M. Lynch is also affiliated with the Northwestern Institute on Complex Systems (NICO). (emails: huanweng@u.northwestern.edu, kmlynch@northwestern.edu).

We thank Paul B. Umbanhowar and Randy A. Freeman for their helpful suggestions and comments.

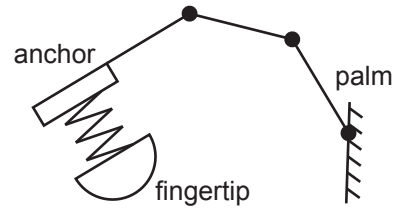

Fig. 2: Simplified model of a finger. The "anchor" is driven by a position-controlled hand and finger joints. The hemispherical fingertip is mounted to the anchor by a 6-dof flexure, providing passive compliance for safe manipulation of rigid objects.

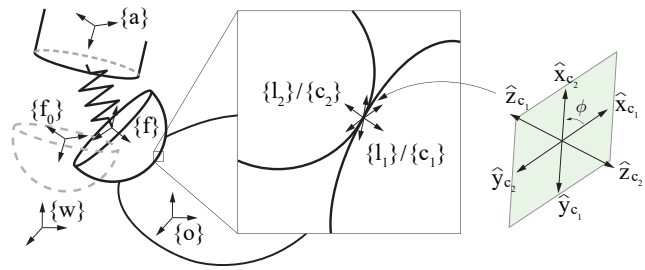

Fig. 3: A fingertip displaced and making contact with an object, with defined frames. The fingertip's initial pose, when the flexure is at rest, is drawn in grey. All the frames at the contact point have their z-axes normal to the tangential plane in green. ϕ is the rotation angle along z-axis of frame $\{l_1\}/\{c_1\}$, from x-axis of $\{l_1\}/\{c_1\}$ to that of $\{l_2\}/\{c_2\}$.

Figure 2 illustrates the anchor-fingertip model employed in this paper. The controls are the joint velocities of the robot arm and robot finger, which directly translate to the velocity of the "anchor" of each finger. The anchor is connected to the fingertip via a 6-dof flexure, providing passive compliance for safe manipulation of rigid objects. The fingertip motion over an external object is determined by the controlled motion of the anchor, the compliance of the flexure, and friction at the contact. For most of our modeling efforts, we assume a quasistatic model (inertial forces are negligible) and that the fingertip contact is a point governed by dry Coulomb friction. Also, in this paper, "rolling" includes all non-sliding motions, including pure rolling, pure spinning, and their combination, because all these cases have no relative linear velocity between contacts on the object and fingertip, and they share a similar mechanics analysis.

II. Contact model and preliminaries

A. Contact model

Figure 3 illustrates a moving compliant fingertip making a point contact with a moving object. A local surface patch and

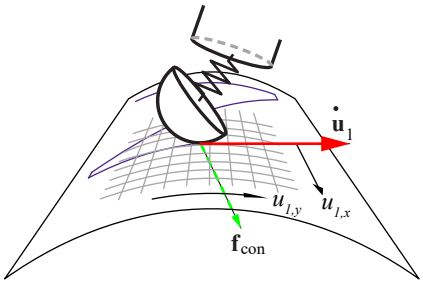

Fig. 4: (Left) A compliant fingertip moving along an "N"-shaped trajectory over the object surface while applying the contact force $\mathbf{f}_{\text{con}}$. A local surface patch and a coordinate frame is defined with the origin at the contact point and two axes $u_{1,x}$ and $u_{1,y}$ orthogonal to each other. The contact point velocity can be represented in that frame as $\dot{\mathbf{u}}_1$.

TABLE I: Frame definitions

Frame	Definition
{w}	World frame.
{o}	Object frame, attached to the object.
{p}	Palm frame, attached to the robot hand palm.
{a}	Anchor frame, attached to the finger anchor, connected with {p} through finger links (phalanges) and joints.
{f}	Fingertip frame, attached to the hemispherical fingertip, connected with {a} through the flexure.
$\{f_0\}$	Fingertip rest frame, attached to {a} but coincident with {f} when the flexure is at rest.
$\{l_1\}$,$\{l_2\}$	Local contact frames at the current contact points, attached to {o} and {f} respectively, each with its z-axis pointing outwards and x, y-axes tangential to the local coordinate system of the surface patch.
$\{c_1\}$,$\{c_2\}$	Moving contact frames at the contact points, attached to the moving contact on the object and fingertip and simultaneously coincident with $\{l_1\}$ and $\{l_2\}$ respectively.

coordinates with orthogonal axes $u_{1,x}$ and $u_{1,y}$ are defined at the contact point on the object to represent the contact velocity $\dot{\mathbf{u}}_1$ along the object surface [3], as an example shown in Figure 4. Using the definitions in [3] and the finger spring compliance model in [2], we define frames as listed in Table I, and an extra index $i = 1 \dots n$ is used in subscripts when $n > 1$ fingers are involved.

B. Notation

Vectors are written in bold lowercase letters, except for poses represented in exponential coordinates $\mathcal{X}$, twists $\mathcal{V} = (\mathbf{v}, \boldsymbol{\omega}) \in \mathbb{R}^6$, and wrenches $\mathcal{F} = (\mathbf{m}, \mathbf{f}) \in \mathbb{R}^6$. Matrices are in bold capital letters and scalars are italicized. All variables are expressed in the world frame {w} unless noted otherwise in the superscripts, and other descriptions are noted in the subscripts. For example, $\mathcal{V}_{\text{wo}}$ indicates the twist of the object frame relative to the world frame, expressed in the world frame, and $\mathcal{V}^{\text{o}}_{\text{wa},2}$ indicates the twist of the anchor frame of finger 2 relative to the world frame, expressed in the object frame.

C. Contact kinematics and mechanics

Using the modeling described above, the contact kinematics and mechanics are derived in the Supplementary Material. Relevant quantities include $\mathcal{F}_{\text{ext}}$, the wrench applied to the object by contact with the environment; $\mathbf{V}_{\text{f\&o}}$, the concatenation of the twists of the n fingertips and the object, relative to the world frame, into a single vector of length $6(n+1)$; $\mathbf{K}_{\text{spr},i}$, the 6×6 stiffness matrix of the flexure at fingertip i; $\mathbf{W}_{\text{con},i}$, the 6×6 representation of the contact wrench exerted by fingertip i on the object; $\boldsymbol{\beta}$, a vector consisting of anchor twists and the rate of change of fingertip contact wrenches; and $\boldsymbol{\Omega}_{\text{f\&o}}$, which satisfies $\boldsymbol{\Omega}_{\text{f\&o}}\mathbf{V}_{\text{f\&o}} = \boldsymbol{\beta}$.

III. Control of In-Hand Rolling Manipulation

The feedforward-feedback in-hand rolling manipulation control algorithm is shown in Figure 5. The feedforward command is derived in Section III-A, which uses finger joint angles $\boldsymbol{\Theta}_{\text{fin}}$, vision feedback of the object pose $\mathbf{T}_{\text{wo}}$, and Visiflex tactile sensor contact location $\mathbf{T}_{\text{ac2},i}$ and wrench $\mathcal{F}^{\text{a}}_{\text{con},i}$ feedback to map the desired twist of the object and the desired rate of change of the wrench applied by the object to the environment to commanded joint velocities of the fingers (and optionally the robot arm). These commanded joint velocities are integrated to create commanded joint positions that are tracked by a PD torque controller and gravity compensation.

A. Feedforward control

Based on Equation (23) in the Supplementary Material, in the usual case that $\boldsymbol{\Omega}_{\text{f\&o}}$ is invertible, the object twist $\mathcal{V}_{\text{wo}}$ as a function of the commanded finger anchor twists $\mathcal{V}_{\text{wa},i}, i = 1 \dots n$ is

$$\begin{aligned}\mathcal{V}_{\text{wo}} &= \begin{bmatrix}\mathbf{0}_{6\times6n} & \mathbf{I}_{6\times6}\end{bmatrix}\mathbf{V}_{\text{f\&o}} = \begin{bmatrix}\mathbf{0}_{6\times6n} & \mathbf{I}_{6\times6}\end{bmatrix}\boldsymbol{\Omega}^{-1}_{\text{f\&o}}\boldsymbol{\beta} \\ &= \boldsymbol{\Pi}(\boldsymbol{\Omega}_{\text{a}}\mathbf{V}_{\text{a}} - \boldsymbol{\beta}_{\text{ext}}),\end{aligned} \tag{1}$$

where

$$\begin{cases}\boldsymbol{\Pi} := \begin{bmatrix}\mathbf{0}_{6\times6n} & \mathbf{I}_{6\times6}\end{bmatrix}\boldsymbol{\Omega}^{-1}_{\text{f\&o}} \\ \boldsymbol{\Omega}_{\text{a}} := \begin{bmatrix}\begin{bmatrix}\mathbf{C}_1\\ \mathbf{0}_{3\times6}\end{bmatrix} & \cdots & \mathbf{0}_{6\times6} \\ \vdots & \ddots & \vdots \\ \mathbf{0}_{6\times6} & \cdots & \begin{bmatrix}\mathbf{C}_n\\ \mathbf{0}_{3\times6}\end{bmatrix} \\ \mathbf{K}_{\text{spr},1} - \mathbf{W}_{\text{con},1} & \cdots & \mathbf{K}_{\text{spr},n} - \mathbf{W}_{\text{con},n}\end{bmatrix} \\ \mathbf{V}_{\text{a}} := \begin{bmatrix}\mathcal{V}_{\text{wa},1}\\ \vdots \\ \mathcal{V}_{\text{wa},n}\end{bmatrix} \\ \boldsymbol{\beta}_{\text{ext}} := \begin{bmatrix}\mathbf{0}_{6n\times1} \\ \dot{\mathcal{F}}_{\text{ext}}\end{bmatrix}.\end{cases}$$

For a robot arm-plus-hand with n fingers,

$$\mathcal{V}_{\text{wa},i} = \mathcal{V}_{\text{wp}} + \mathcal{V}_{\text{pa},i} = \mathbf{J}_{\text{arm}}\dot{\boldsymbol{\theta}}_{\text{arm}} + \mathbf{J}_{\text{fin},i}\dot{\boldsymbol{\theta}}_{\text{fin},i}, i = 1, \dots, n,$$

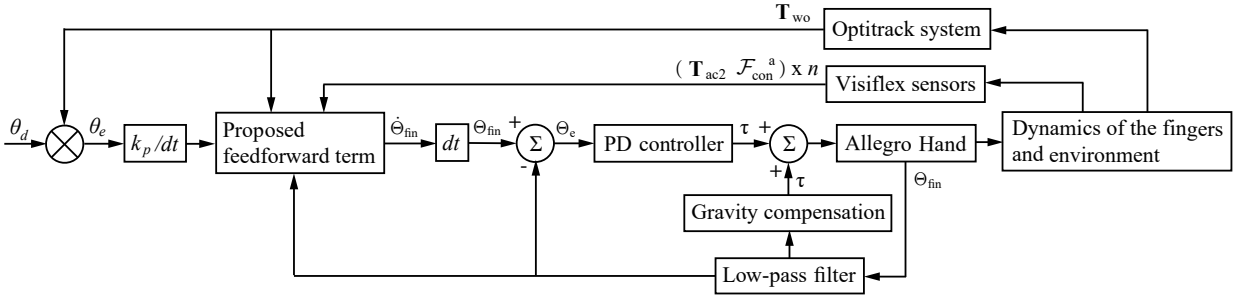

Fig. 5: Control of in-hand compliant rolling manipulation used in experiments. The feedforward term maps the desired object rotation velocity and the desired zero change of the wrench applied by the object to the environment to the commanded finger joint velocities. These commanded joint velocities are integrated to create commanded joint positions that are tracked by a PD torque controller and gravity compensation.

where $\mathbf{J}$ and $\dot{\boldsymbol{\theta}}$ are the Jacobian matrix and joint angles of either the robot arm or a finger. Stacking these equations yields

$$\mathbf{V}_{\text{a}} = \boldsymbol{\Xi}\dot{\boldsymbol{\Theta}},\ \boldsymbol{\Xi} := \begin{bmatrix} \mathbf{J}_{\text{fin},1} & & & \mathbf{J}_{\text{arm}} \\ & \ddots & & \vdots \\ & & \mathbf{J}_{\text{fin},n} & \mathbf{J}_{\text{arm}} \end{bmatrix},\ \dot{\boldsymbol{\Theta}} := \begin{bmatrix} \dot{\boldsymbol{\theta}}_{\text{fin},1} \\ \vdots \\ \dot{\boldsymbol{\theta}}_{\text{fin},n} \\ \dot{\boldsymbol{\theta}}_{\text{arm}} \end{bmatrix}.$$

Substituting into Equation (1) yields

$$\boldsymbol{\Sigma}\dot{\boldsymbol{\Theta}} = \mathcal{V}_{\text{wo}} + \boldsymbol{\Pi}\boldsymbol{\beta}_{\text{ext}},\ \boldsymbol{\Sigma} := \boldsymbol{\Pi}\boldsymbol{\Omega}_{\text{a}}\boldsymbol{\Xi}. \tag{2}$$

The joint velocities $\dot{\boldsymbol{\Theta}}_{\text{opt}}$ are chosen to minimize $||\dot{\boldsymbol{\Theta}}_{\text{opt}}||_2 = \dot{\boldsymbol{\Theta}}_{\text{opt}}^{\intercal}\dot{\boldsymbol{\Theta}}_{\text{opt}}$ while satisfying Equation (2),

$$\dot{\boldsymbol{\Theta}}_{\text{opt}} = \boldsymbol{\Sigma}^{\intercal}(\boldsymbol{\Sigma}\boldsymbol{\Sigma}^{\intercal})^{-1}(\mathcal{V}_{\text{wo}} + \boldsymbol{\Pi}\boldsymbol{\beta}_{\text{ext}}). \tag{3}$$

When the robot arm and hand are stationary ($\dot{\boldsymbol{\theta}}_{\text{arm}} = \mathbf{0}$) and only the fingers move, the optimal joint velocities are

$$\dot{\boldsymbol{\Theta}}_{\text{fin}} = \boldsymbol{\Sigma}_{\text{fin}}^{\intercal}(\boldsymbol{\Sigma}_{\text{fin}}\boldsymbol{\Sigma}_{\text{fin}}^{\intercal})^{-1}(\mathcal{V}_{\text{wo}} + \boldsymbol{\Pi}\boldsymbol{\beta}_{\text{ext}}), \tag{4}$$

where $\boldsymbol{\Sigma}_{\text{fin}} := \boldsymbol{\Pi}\boldsymbol{\Omega}_{\text{a}}\boldsymbol{\Xi}_{\text{fin}}$, $\text{rank}(\boldsymbol{\Sigma}_{\text{fin}}) = 6$, $\dot{\boldsymbol{\Theta}}_{\text{fin}}$ is the stacked vector of $\dot{\boldsymbol{\theta}}_{\text{fin},1}, \cdots, \dot{\boldsymbol{\theta}}_{\text{fin},n}$, and $\boldsymbol{\Xi}_{\text{fin}} = \text{blockdiag}(\mathbf{J}_{\text{fin},1}, \cdots, \mathbf{J}_{\text{fin},n})$.

Equation (3) or (4) provides the feedforward term for control, except under singular configurations and contact wrenches when $\text{rank}(\boldsymbol{\Omega}_{\text{f\&o}}) < 6n+6$, $\text{rank}(\boldsymbol{\Sigma}) < 6$, or $\text{rank}(\boldsymbol{\Sigma}_{\text{fin}}) < 6$.

IV. Experiments

We tested in-hand rolling manipulation using an experimental system consisting of a WAM robot arm, an Allegro four-fingered hand, four Visiflex tactile sensors, and ten Prime^{x} Optitrack cameras. Twisting manipulation similar to what is shown in Figure 1 was tested using a cylindrical object mounted on both a rotational axis and a screw axis (Figure 6). Optical markers were attached to the cylinder for vision tracking. In all experiments, the robot arm, and therefore palm, were held stationary during manipulation, and all manipulation was performed by the fingers only.

Figure 7 shows snapshots of three fingers of the hand performing a twisting operation of the cylinder on a rotational axis. The fingers roll over the cylinder as the operation proceeds. Figure 8 shows the view of one of the tactile sensors: the location of the object contact on the fingertip dome is tracked, and the motions of eight LED fiducials are used to determine the flexure's displacement and therefore the contact wrench from the known flexure stiffness.

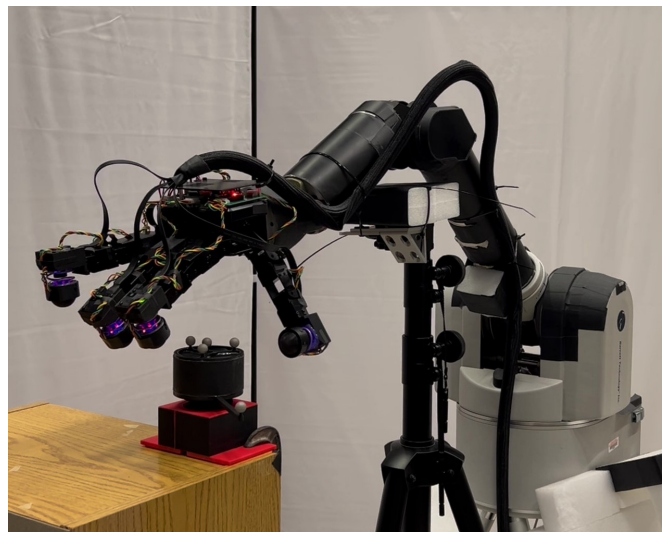

Fig. 6: Snapshot of the robot arm and hand with Visiflex tactile sensors approaching a cylinder to perform screwing manipulation.

We tested both feedforward and feedback control for rotating the cylinder about a rotational axis. The task was to use three fingers to rotate the cylinder by 30° at a constant speed, completing the motion in 5 s. This task requires control of rolling contact over each of the three fingers, as the fingers do not have enough degrees of freedom to complete the task without relative motion at the finger-object contacts. The results of representative sample runs are shown in Figure 9. Each color bar indicates the number of runs left that maintain the grasp throughout the motion. Effects such as imperfect modeling, backlash, and friction in the fingers cause the fingers to occasionally slip on the cylinder with feedforward control only, but these issues are largely mitigated by the full feedback control scheme in Figure 5, and tracking errors were small.

A similar experiment was performed for the cylinder mounted on a screw axis, and the results are reported in Figure 10.

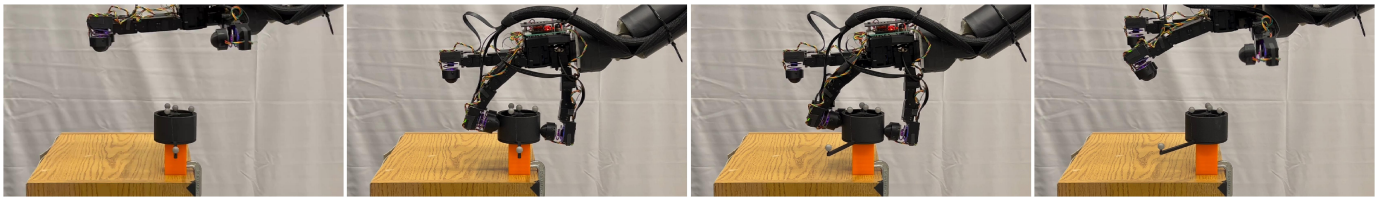

Fig. 7: Snapshots of rotating the cylinder on the axial support.

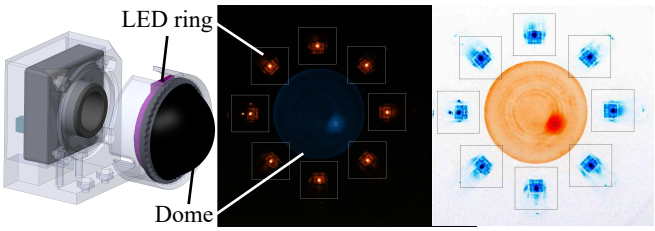

Fig. 8: (Left) Schematic of the Visiflex tactile sensor. (Middle) The embedded camera detects the contact location on the dome and the deflection of the eight LED fiducials, which allows calculation of the contact wrench due to the known flexure stiffness. (Right) A color-adjusted version of the camera's view.

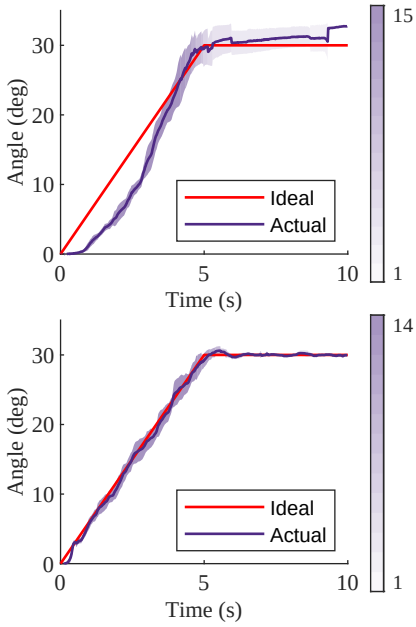

Fig. 9: Experimental results of rotating the cylinder with feedforward only (top) and feedback (bottom) control. Each color bar indicates the number of runs that maintain the grasp throughout the motion.

V. Conclusion

This paper presents (1) the contact mechanics of in-hand rolling manipulation with compliant tactile-sensing fingertips, (2) a controller that uses the contact equations to stabilize rolling manipulation, and (3) preliminary experimental validation. The rolling manipulation controller takes advantage of the contact location and wrench information provided by the Visiflex compliant tactile sensors. Future work includes (1) a more systematic experimental evaluation of the capability of the model-based in-hand rolling manipulation controller on more challenging manipulation tasks and (2) exploration of integration of the strengths of the model-based approach with the strengths of data-driven methods.

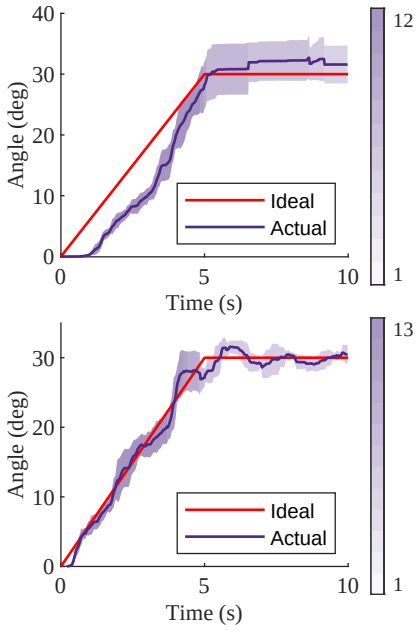

Fig. 10: Experimental results of screwing with feedforward only (top) and feedback (bottom) control. Each color bar indicates the number of runs that maintain the grasp throughout the motion.

References

[1] A. J. Fernandez, H. Weng, P. B. Umbanhowar, and K. M. Lynch, "Visiflex: A low-cost compliant tactile fingertip for force, torque, and contact sensing," *IEEE Robotics and Automation Letters*, vol. 6, no. 2, pp. 3009–3016, 2021.

[2] J. Shi, H. Weng, and K. M. Lynch, "In-hand sliding regrasp with spring-sliding compliance and external constraints," *IEEE Access*, vol. 8, pp. 88 729–88 744, 2020.

[3] D. J. Montana, "The kinematics of contact and grasp," *The International Journal of Robotics Research*, vol. 7, no. 3, pp. 17–32, 1988.

[4] K. M. Lynch and F. C. Park, *Modern Robotics*. Cambridge University Press, 2017.